ACS Catalysis

Research Article

pubs.acs.org/acscatalysis

Catalytic Transformations of Birch Kraft Pulp

Mats Käldström,[†] Narendra Kumar,[†] Mikko Tenho,[‡] Maksim V. Mokeev,[§] Yulia E. Moskalenko,[§] and Dmitry Yu. Murzin*,[†]

[†]Laboratory of Industrial Chemistry and Reaction Engineering Process Chemistry Centre, Åbo Akademi University, FIN-20500 Åbo/Turku, Finland

[‡]Laboratory of Industrial Physics, Department of Physics and Astronomy, University of Turku, FI-20014 Turku, Finland

[§]Spectroscopy Group, Institute of Macromolecular Compounds RAS, 199004 Saint-Petersburg, Bolshoy pr. 31, Russia

Supporting Information

ABSTRACT: The goal of the work was to investigate hydrolysis and hydrogenation of a mixture of cellulose and hemicelluloses. Hydrolysis and hydrolytic hydrogenation of bleached birch (betula) kraft pulp from a Finnish pulping mill and microcrystalline cellulose (Aldrich) into sugars and sugar alcohols was carried out in the liquid phase in a batch mode under 20 bar of hydrogen at 458 K. Proton forms of different microporous and mesoporous materials, Pt modified MCM-48, MCM-41 mesoporous material, and Pt on Al_2O_3 were used in the catalytic experiments. The conversion of cellulose and hemicelluloses was dependent on the type of zeolite structure, strength of active sites, their number, and presence of metal. The ratio of formed monomers/dimers varied because of the pore size of the used catalyst. The yields of the main products, for example, sugars, sugar alcohols, and furfurals (xylose, glucose, xylitol, sorbitol, furfural, furfuryl alcohol, and 5-hydroxymethyl furfural), were shown to depend on the type of substrate as well as on the active sites, acidity, presence of metal, and structure of the zeolite and mesoporous material.

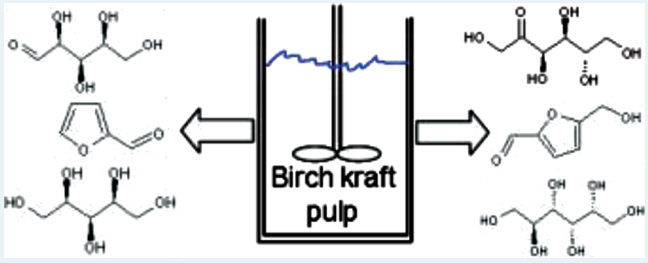

KEYWORDS: *cellulose, hydrolysis, hydrogenation, glucose, xylose, xylitol, sorbitol*

1. INTRODUCTION

Catalysis aimed at the utilization and processing of biomass and development of tailor-made catalytic materials, as well as novel catalytic processes involving unconventional solvents, has become an important research area in recent years.[1] Being the most abundant organic compound in the world, valorization of cellulose will most certainly play one of the main roles in the utilization of the renewables. Lignocellulosic biomass is an excellent raw material for these processes since the utilization of the biomass does not compete with the food production. Typically lignocellulosic biomass refers to wood, generally consisting of about 40−50% cellulose, 23−33% lignin, and 25−35% of hemicelluloses.[2] As cellulose comprises glucose units, the hemicelluloses are composed of different monomeric units, depending on the type of biomass.

The feedstock can be treated in different ways at an initial stage of biomass utilization, for example, through gasification, pyrolysis, fermentation, and hydrolysis.[3] The hydrolysis of cellulose has, however, recently been mentioned to be the most important entry point into a biorefinery scheme based on carbohydrates.[4] The first technology for the acid hydrolysis of cellulose was the Scholler process which was developed in the 1920s in Germany.[5]

The first detailed kinetic study of cellulose hydrolysis made in 1935 reports that the hydrolysis rate, in H_2SO_4, decreases significantly as the degree of polymerization (DP) of the polymer increases.[4] Catalytic upgrading of cellulose into sugars and sugar alcohols over heterogeneous catalysis has gained a lot of interest in the recent years, and several research groups have reported the valorization of cellulose into chemicals in aqueous media through hydrolytic hydrogenation.[6−11] Some reports concerning real feedstock upgrading, such as spruce chips and sugar beet fiber, have also recently been published.[12,13]

The first step in hydrolytic hydrogenation of cellulose is the hydrolysis into glucose and oligomers, followed by the second step, hydrogenation of the free sugars on the active sites on the metallic catalyst into polyols.[4,14] This process is attractive since it converts cellulose into sugars and sugar alcohols in a one-pot procedure using water as a solvent at elevated temperatures and in the presence of hydrogen.

Aluminosilicates are important catalysts in the upgrading of fossil fuels, catalyzing such reactions as bond breaking, cracking, and alkylation, and they also might have an application in the upgrading of biomass and refinement processes of sugars.[15−18] Through their shape-selectivity, they can favor reaction pathways that give desired products. Furthermore, they are easy to reuse and recover, and the application of these heterogeneous catalysts follows the principles of sustainability

Received: September 14, 2011
Revised: May 26, 2012
Published: May 29, 2012

   dx.doi.org/10.1021/cs2006839 | ACS Catal. 2012, 2, 1381−1393

and green chemistry. Not all experience gained in the transformation of hydrocarbons during the last 100 years, however, can be directly transferred to biomass conversion.[1] New process design and courageous innovations are needed in the development of advanced biorefineries for production of chemicals and fuels in a sustainable manner.

In this work we report the transformation of bleached birch (betula) kraft pulp containing, for Finnish pulping mills, a typical mixture of hemicelluloses and cellulose, and pure cellulose into sugars and sugar alcohols over zeolites and Pt modified mesoporous materials, and for comparison Pt on Al_2O_3. Mesporous materials were chosen because of their large pores and low acidity. The catalytic performance with respect to catalyst structure and acidity was investigated. The use of mesoporous materials in catalysis has recently been reported by several groups.[19,20] The novelty of the current study lies in the utilization of real feedstock, in the form it is produced in biorefineries, containing a mixture of cellulose and hemicelluloses. Geboers et al. recently pointed out the importance to perform catalytic experiments using real feedstock,[21] and most of the articles we have encountered report the use of pure cellulose and not real feedstock, which would be used in upgrading processes in industrial scale.

2. EXPERIMENTAL SECTION

2.1. Catalyst Synthesis and Characterization. *2.1.1. Synthesis of H-MCM-22 Zeolite.* Na-MCM-22 microporous molecular sieve with three different acidities was synthesized according to the procedure described elsewhere[22−25] with some modifications. The synthesis of the zeolite was carried out using the following procedure: water and sodium aluminate (Riedel-de Haën, purity ≥95%) were added to sodium hydroxide (Merck, purity ≥99%), and the mixture was stirred for 10 min. After stirring, hexamethyleneimine (Aldrich, purity 99%) and fumed silica (Aldrich, purity 99.8%) were added, and the blend was stirred for another 20 min. The acidity of the zeolite was tilted by changing the concentration of the reactants. After forming a homogeneous phase, the mixture was transferred to Teflon cups and inserted into autoclaves. The synthesis was carried out at 423 K for 7 days. After completion of synthesis, the material was filtered, washed with distilled water to neutral pH, dried at 373 K, and calcined at 823 K for 8 h.

2.1.2. Synthesis of SBA-15 Mesoporous Material. Synthesis of SBA-15 was performed in a 300 mL autoclave (Parr Instruments) by using the methods mentioned by Zhao et al., Kumaran et al., and Aguado et al.[26−28] with some modifications. The reagents used in the synthesis were Pluronic P123 (BASF) coblock polymer, hydrochloric acid (Merck), TEOS (Merck), aluminum isopropoxide (Merck), and distilled water. The prepared gel was introduced in a Teflon cup and inserted into a 300 mL autoclave. The synthesis was carried out at 373 K followed by washing of the material obtained with 1000 mL of distilled water, drying at 373 K for 12 h, and calcination at 773 K.

2.1.3. Synthesis of H-MCM-41 Mesoporous Material. The synthesis of Al-MCM-41 was carried out as described by Kresge et al.[29] and Bernas et al.[30] with some modifications. Synthesis of the Na-MCM-41 mesoporous molecular sieve was carried out in a 300 mL autoclave. The synthesis was performed by preparing solutions A, B, and C. Solution A was prepared by mixing fumed silica (Aldrich) with distilled water under continuous stirring. Solution B was made by adding tetramethylammonium silicate (Sachem) to sodium silicate (Merck) and stirring for 15 min. Solution C was prepared by dissolving tetradecyl trimethyl ammonium bromide (Aldrich) in distilled water. Solution B was added to solution A slowly and stirred for 20 min; subsequently, solution C was introduced under vigorous stirring. A required amount of aluminum isopropoxide (Aldrich) was mixed, and the gel solution was stirred for 30 min. After measuring pH of the prepared gel, it was introduced in a Teflon cup, which was inserted into an autoclave. The synthesis was performed at 373 K in an oven. After completion of the synthesis, the reactor was quenched and the mesoporous material was filtered and washed thoroughly with distilled water. The synthesized mesoporous Na-MCM-41 was dried at 383 K and calcined at 823 K. The Na-MCM-41 mesoporous material was ion-exchanged with aqueous solution of ammonium chloride for 24 h, followed by washing with distilled water, drying at 373 K, and calcination at 773 K to obtain H-MCM-41.

2.1.4. Synthesis of Pt-MCM-41 Mesoporous Material. Preparation of 8 wt % Pt-MCM-41 catalyst was done by the evaporation impregnation method using aqueous solution of hexachloroplatinic acid. The catalyst was dried at 373 K and calcined at 673 K after the impregnation. The metal modified catalyst was reduced at 623 K for 2 h under flowing hydrogen gas prior to testing.

2.1.5. Synthesis of H-MCM-48 Mesoporous Material. Synthesis of Al-MCM-48 was carried out by using the method described by Pu et al.[31] with some modifications. To a solution of NaOH and cetyl trimethyl ammonium chloride (CTMACl) in distilled water aluminum isopropoxide (AIP) was added and stirred for 15 min to allow the hydrolysis of AIP. Then, tetraethyl orthosilicate (TEOS) was added and stirred in an open vessel at room temperature for 1 h to achieve complete hydrolysis of TEOS. The pH of the mixture was measured. The gel was transferred into a 300 mL autoclave; thereafter the synthesis was carried out at 373 K for 75 h. Na-MCM-48 was ion-exchanged with an ammonium chloride solution for 48 h, washed with distilled water, dried, and calcined to obtain H-MCM-48.

2.1.6. Synthesis of Pt-H-MCM-48-IS Catalyst. Pt modified MCM-48 mesoporous material was synthesized using the in situ method by adding aqueous solution of hexachloroplatinic acid with the gel solution prepared for synthesis of MCM-48. The synthesis was carried out following a procedure similar to that of Al-MCM-48. After completion of synthesis Pt-MCM-48-IS was washed thoroughly with distilled water, dried at 373 K, and calcined.

2.1.7. Synthesis of Pt-H-MCM-48-IE Catalyst. Pt modified MCM-48 mesoporous material was prepared using an ion-exchange/adsorption method. H-MCM-48 was introduced in a beaker containing hexachloroplatinic acid and stirred for 48 h. The Pt-MCM-48 catalyst was filtered, dried at 373 K, and calcined in a muffle oven at 673 K.

2.1.8. Pt on Al_2O_3 Catalyst. 4.4 wt % Pt on Al_2O_3 was purchased from Degussa and reduced at 623 K for 2 h under flowing hydrogen gas prior to the catalytic testing.

2.1.9. Catalyst Characterization. The specific surface area of fresh catalysts was measured by the nitrogen adsorption method (Sorptometer 1900, Carlo Erba Instruments). The catalysts were outgassed at 423 K prior to the measurement and, depending on the catalysts, Dubinin as well as the Brunauer−Emmett−Teller (BET) equations were used to calculate the specific surface area.

dx.doi.org/10.1021/cs2006839 | ACS Catal. 2012, 2, 1381−1393

The acidity of the synthesized mesoporous materials was measured by infrared spectroscopy (ATI Mattson Infinity spectrometer) by using pyridine (≥99.5%, a.r.) as a probe molecule for qualitative and quantitative determination of both Brønsted and Lewis acid sites. The FTIR spectrometer was equipped with an in situ cell containing ZnSe windows. The samples were pressed into thin self-supported discs (weight 15−20 mg and radius 0.65 cm). Pyridine was first adsorbed for 30 min at 373 K and then desorbed by evacuation at different temperatures (523, 623, and 723 K) to obtain a distribution of acid site strengths. All spectra were recorded at 373 K with a spectral resolution equal to 2 cm^{-1}. Spectral bands at 1545 and 1450 cm^{-1} were used to identify the Brønsted (BAS) and Lewis acid sites (LAS). The amounts of BAS and LAS were calculated from the intensities of corresponding spectral bands using the molar extinction coefficients reported by Emeis.[32]

The metal dispersion was determined from the amount of chemisorbed CO by a pulse method. The experiments were carried out using a Micromeritics TPD/TPR 2910 AutoChem instrument. The sample (~0.170 mg) was inserted into a quartz U-tube and was reduced with H_2 stream (AGA, 9.9999%, 20 mL/min). A ramp rate of 5 K/min was applied, and the temperature was linearly raised to the final temperature of 623 K; thereafter it was held for 120 min. The sample was then cooled to 313 K under flowing He (AGA, 99.999%), and the experiment started once the baseline was stable. CO (AGA, 10% in He) was introduced, and the pulses were repeated until complete saturation. The stoichiometry of CO/Pt was 1.[33,34]

The metal loading was determined by ICP-OES. Approximately 0.1 g of sample was inserted into a Teflon bomb, 4 mL HF, 1 mL of HCl, and 0.5 mL of HNO_3 were added. The zeolite was dissolved in a microwave oven and diluted with deionized water to decrease the HF concentration.

X-ray powder diffractiometer (Philips PW 1820) was applied to study the structure and phase purity of MCM-48 mesoporous material, whereas scanning electron microscope (Leica) was used to investigate the morphology of the material.

The zeolite framework was analyzed by solid state NMR. Spectra were recorded under magic angle spinning (MAS) at ambient temperature on Bruker spectrometers Avance-400 and Avance II-500. Samples were packed in a 4 mm zirconium rotor and spun at a 10−13 kHZ frequency. Single pulse ^{29}Si spectra were acquired at 79.4 or 99.4 MHz, respectively, using 4 μs pulse with 10 s repetition time. Single-contact $^{1}H \rightarrow ^{29}Si$ cross-polarization (CP) technique with 6 ms contact time was applied for ^{29}Si CP-spectra recording. For ^{27}Al NMR at 104.2 or 130.2 MHz, respectively, 0.7 or 3.1 μs pulse was used with repetition time of 0.5 s. Reference samples employed were Q_8M_8 for ^{29}Si and $Al(H_2O)_6Cl_3$ for ^{27}Al. Deconvolution of the spectra obtained was performed by the use of DMFIT software.[35]

2.2. Pulp and Cellulose Characterization. The degree of polymerization of the kraft pulp was estimated by viscosity measurements in cupriethylenediamine solution.[36,37] Free monosaccharide content of the pulp was checked according to the following procedure: 64 mg of the dry pulp was put in a tube along with 10 mL of deionized water: the suspension was stirred and left overnight, thereafter the water was filtered and analyzed by HPLC and silylation GC-MS. The hemicelluloses were determined by acid methanolysis and GC.[38] The pulp was freeze-dried, and about 7 mg was subjected to acid methanolysis by 2 mol/L HCl in anhydrous methanol to reduce noncellulosic polysaccharides into their monomeric sugar units. After 5 h at 373 K the samples were neutralized with pyridine, and sorbitol was added as an internal standard. Part of the clear sample was transferred to a new flask and dried, silylated, and analyzed by GC.

X-ray powder diffraction (Philips PW 1820) and thermogravimetrical analysis (TGA) were applied to study the structure of the fresh cellulose powder and both initial and treated birch kraft pulp. The TGA analysis was performed using a Cahn D-200 digital recording balance under the flow of synthetic air. The following temperature program for the oven was used: heating 2 K/min from 298 to 873 K and dwelling at 873 K for 180 min.

2.3. Catalytic Experiments. The catalytic and noncatalytic experiments were performed in a 300 mL Parr autoclave connected to a prereactor with a volume of 200 mL. The autoclave was provided with a 0.5 μm filtered sampling outlet, which prevented the catalyst particles to pass through it. The temperature was measured with a thermocouple and controlled automatically (Brooks Instrument). In a typical experiment 0.64 g of dry bleached birch kraft pulp from a Finnish pulp mill or pure cellulose (Aldrich) was mixed in 150 mL of deionized water along with 0.30 g of catalyst with a particle size <63 μm. Furthermore, some catalytic experiments with D-(-)-fructose (Sigma-Aldrich ≥99%) and D-(+)-glucose (anhydrous, Acros Organics) were performed for better understanding of the reaction pathways taking place. In the experiments with the model compounds the same amounts of substrate and catalyst were used as in the experiments with cellulose and kraft pulp. The procedure in the noncatalytic experiments was the same as in the catalytic experiments except that no catalyst was added in the former. To get the small particle size, for avoiding internal diffusion limitations, zeolite catalysts were crushed and sieved. The hydrogen pressure of 20 bar was applied, and the solution was heated to 458 K. The stirring rate was 1145 rpm to eliminate external diffusion. When the reactor had reached its set temperature, stirring was applied, and this was considered as the initial reaction time. Liquid samples were taken at different times and analyzed with an HPLC equipped with an HPX-87C as well as a HPX-87H column.

2.4. Product Analysis. *2.4.1. Analysis of Monosaccharides and Low Molecular Weight Compounds.* Quantitative analysis of the oxygenated species was carried out. The samples taken from the reaction were analyzed chromatographically with Aminex HPX-87C and Aminex HPX-87H columns. The HPX-87C column was connected to a refractive index (RI) detector with a diluted calcium sulfate solution ($CaSO_4$, 1.2 mM) as a mobile phase. The flow was 0.4 mL/min, and the temperature was set to 353 K. Low concentrated sulphuric acid (0.005 M) was used as a mobile phase in the Aminex cation H+ column, the flow was 0.5 mL/min, and the temperature was set to 338 K. The samples were injected into the HPLC directly after the experiments without any pretreatment other than filtering to prevent solid particles from entering the columns. Several different concentrations of various standards were made and analyzed with HPLC. The standards were purchased from Aldrich or Fluka and had a purity of ≥99%. The HPLC was calibrated with the different standards which made it possible to calculate the yields of the products.

2.4.1.1. Analysis of Volatile Compounds. The volatile compounds were analyzed with GC/MS and headspace solid phase micro extraction (SPME). Two milliliters of the solution containing the reaction products were transferred into a small 4 mL flask equipped with a rubber cap. The sample flask was

dx.doi.org/10.1021/cs2006839 | ACS Catal. 2012, 2, 1381−1393

heated to 320 K. The needle with the fiber penetrated into the bottle through the cap, and the fiber was exposed to the headspace of the sample for 30 min. The fiber used for extraction was coated with carboxen/polymethylsiloxane (CAR/PDMS). The components were enriched on the surface when equilibria were reached between the headspace and the fiber; thereafter the syringe was injected into the GC-MS for analysis. The inlet chamber was set on 543 K, where the absorbed and adsorbed analytes were thermally desorbed in the hot injector of the gas chromatograph. The time of desorption was 10 min which was sufficient to ensure total desorption; moreover, no memory effect was observed as the same fiber was inserted for a second time. The GC/MS was equipped with a capillary column (DB-Petro 50 m × 0.2 mm × 0.5 μm). The following temperature program was used: dwelling for 10 min at 313 K, heating 0.9 K/min to 348 K followed by heating 1.1 K/min to 393 K, heating 10 K/min to 473 K and dwelling at 473 K for 20 min.

2.4.1.2. Silylation-GC-MS. For making the sugars volatile and suitable for GC-analysis, the samples were silylated. A 500 μL portion of the liquid samples after 24 h of reaction time were transferred to a test tube and dried in a water bath operating at 313 K under nitrogen flow. A blank sample containing only distilled water was dried as a reference. The dried samples were silylated by addition of 100 μL of pyridine (Fluka, >99%), 200 μL of hexamethyldisilazane (Fluka, >98%), and 100 μL of chloromethylsilane (Fluka, >98%). The samples were stirred and left overnight. Thereafter, the samples were transferred into small ampules and analyzed with GC-MS. The GC-MS was equipped with an HP-1 column (25 m × 0.2 mm × 0.11 μm), and the following temperature program was used: dwelling at 333 K for 0.25 min and heating to 573 K with the heating rate 6 K/min.

2.4.2. Analysis of Oligomers. Two milliliters of the liquid samples were freeze-dried and redissolved in 1.0 mL of a 1:1 mixture of pyridine and acetic anhydride. The samples were left reacting for three days in the dark and shaken at least once a day. Approximately the same amount of ethanol as the anhydride-pyridine mixture was added to the samples, and the solvents were evaporated under a stream of nitrogen until dry. The samples were further dried in vacuum desiccator. The dry samples were dissolved in tetrahydrofuran (THF) to a known concentration; thereafter, they were filtrated and analyzed with HPLC. A standard solution was also prepared by dissolving a known amount of A-D-glucose-penta-acetate and D-cellubiose-octa-acetate in 50 mL of THF. The standard solution was analyzed together with the other prepared samples. The chromatograph was equipped with a Jordi Gel DVB 500A (300 mm × 7.8 mm) column operating at a temperature of 40 °C, THF was used as an eluent, and the flow through the system was 0.8 mL/min.

2.4.3. pH. The pH of the solution was measured after the reaction was stopped.

2.4.4. Total Organic Carbon. To determine the total amount of dissolved cellulose, that is, liquid products, the total organic carbon (TOC) was measured. The samples were analyzed with a total organic carbon analyzer, TOC-VCSN, from Shimadzu Corporation.

3. RESULTS

3.1. Catalyst Characterization Results. *3.1.1. X-ray Powder Diffraction and Scanning Electron Microscopy.* Most of the synthesized materials were analyzed by X-ray powder diffraction (XRD) and/or scanning electron microscopy (SEM). The results have, however, been published recently and are thus omitted here.[39−41]

3.1.2. Acidity. The zeolitic materials exhibited much higher acidity than the mesoporous materials with MCM-22-30 being the most acidic, as expected theoretically (Table 1).

Table 1. Acid Sites of the Catalyst Used

	Brønsted acid sites (μmol/g)			Lewis acid sites (μmol/g)		
catalyst	523 K	623 K	723 K	523 K	623 K	723 K
H-MCM-22-30*	277	242	173	90	40	15
H-MCM-22-50*	207	191	141	47	19	5
H-MCM-22-70*	178	168	81	36	11	2
H-MCM-48	59	18	2	63	25	7
Pt-MCM-48-IS	39	6	5	62	6	3
Pt-MCM-48-IE	45	3	2	43	2	1
Al-SBA-15	17	8	4	41	13	4
H-MCM-41	26	11	3	40	20	12
Pt-MCM-41						
Pt-Al_2O_3						

*Indicate silica to alumina ratio.

The number of Brønsted acid sites was considerably higher in the microporous than in the mesoporous materials whereas the amounts of Lewis acid sites were quite similar for the two types of catalysts. Among the different MCM-48 mesoporous materials the proton form was the most acidic, and introduction of Pt into the structure caused some decrease in Brønsted acidity, while no considerable changes were seen in the Lewis acidity.[42,43] Because of the high metal content, leading to low transparency of the materials, it was not possible to determine the acidity of Pt-Al_2O_3 and Pt-MCM-41 by the transmission spectroscopy method.

3.1.3. Surface Area. The surface area and the metal loading data are shown in Table 2. Introduction of the metal by ion exchange (Pt-MCM-48-IE) resulted in a substantial decline of surface area, which could partly be explained by large size Pt particles blocking the pores after calcination. The magnitude of this decline is, however, surprisingly drastic compared to the amount of introduced Pt. The drastic decrease in surface area is likely accounted for the partial collapse of the material structure. Comparing the pore specific volumes of the three

Table 2. Surface Area, Pore Specific Volume, and Metal Loading of the Tested Catalysts

catalyst	surface area (m^2/g), BET	pore specific volume (cm^3/g)	metal loading (wt %)	metal dispersion (%)	metal particle diameter (nm)
H-MCM-48	941	0.71			
Pt-MCM-48-IS	1213	0.49	0.4	10	11
Pt-MCM-48-IE	557	0.37	0.1	14	8
Al-SBA-15	828				
H-MCM-41	951				
Pt-MCM-41	873		8.0	23	5
Pt-Al_2O_3	270		4.4	53	2
			surface area (m^2/g), Dubinin		
H-MCM-22-30			601		
H-MCM-22-50			642		
H-MCM-22-70			551		

dx.doi.org/10.1021/cs2006839 | ACS Catal. 2012, 2, 1381−1393

MCM-48 materials, one can also notice that the pore volume of the exchanged material (Pt-MCM-48-IE) is by far the lowest (Table 2). A decline in the surface area was also observed when MCM-41 was loaded with Pt by impregnation. The Pt-MCM-48-IS mesoporous material exhibited the highest surface area, even higher than the proton form of the catalyst. The high surface area may be attributed to the formation of micropores at the expense of the mesopores during calcination, which is evident from the pore specific volumes seen for the compared materials (Table 2). The metal loading of the samples is, furthermore, quite low taking into account that the nominal loading was 2 wt %. The introduction of the metal was performed by excess of hexachloroplatinic acid (H_2PtCl_6), when the metal is in the anionic form. The surface area of the different MCM-22 zeolites was around 600 m^2/g, which is very typical for the MWW type zeolite.[44]

3.1.4. NMR Spectroscopy. The ^{27}Al spectra of zeolites show two sets of signals: at 0 ppm, corresponding to octahedral Al (Al(VI)), and a broader band at about 55 ppm due to 4-coordinated framework Al (Al(IV)). The presence of a signal Al(VI) pinpoints that aluminum is not fully incorporated in the zeolite structure, as after calcinations extra framework species are present. In Table 3 the contributions of octahedral and

Table 3. Specification of Al in the Catalysts Studied by NMR

sample	Al(IV)/Al(VI)	Al(IV)	Al(VI)
SBA-15	7.4	88.1	12.0
MCM-22-30	5.1	83.6	16.4
MCM-22-50	7.9	88.7	11.3
MCM-22-70	3.9	73.2	26.8
MCM-48	7.4	88.0	12.0
Pt-MCM-48-IS	12.1	92.4	7.6
Pt-MCM-48-IE	3.1	75.5	24.5

tetrahedral Al are given. It is worth noting that the smallest amount of Al (VI) was observed in Pt-MCM-48-IS, while for SBA-15 this signal is very broad indicating certain degree of amorphousness. In addition the absolute Al content was the lowest in this material among the samples listed in Table 3.

The signal of Al(IV) in fact corresponds to several tetrahedral Al sites in the zeolite structure. For MCM-22 it was possible to fit the signal at 56 ppm with the peaks present in Figure 1. Numerical values of the peaks, corresponding to Si−O−Al angles and population (as normalized integral intensities reflecting the number of Al atoms in distinct crystallographic sites) are presented in the Table 4.

In the ^{29}Si spectra a broad, well structured signal in Q3-Q4 region was observed. For MCM-22 it was possible to distinguish 5 signals in Q4 environment and a signal in Q3, which most probably corresponded to silanol groups $Si(OSi)_3OH$ and $Si(OSi)_2(OH)_2$. The amount of these defects was in the range of 7−12%. The chemical shifts assignments, coordination and integral intensities are listed in Table 5.

The position of lines in the spectra is determined by the substitution of Al in the coordination sphere Q4 and is accompanied by a shift to the lower field. There is a clear correlation between the chemical shift and the angle in Si−O−Al.[45]

$$\delta = -0.6192\alpha - 18.68 \quad (1)$$

Following the model reported by Leonowicz et al., the shifts and population for MCM-22 (as normalized integral values

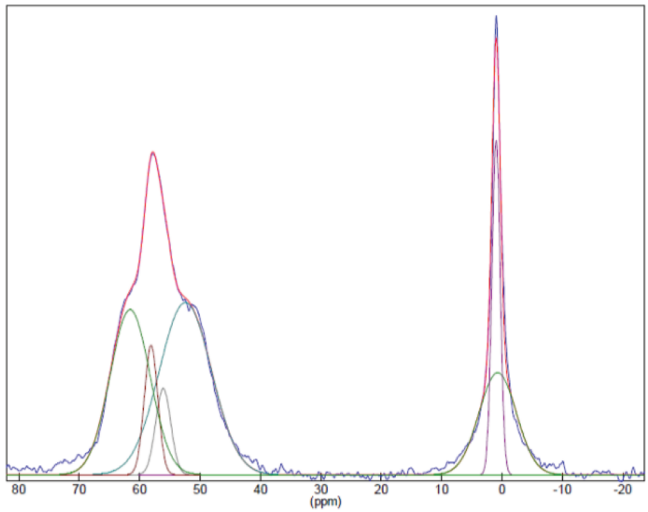

Figure 1. Deconvolution of ^{27}Al NMR spectra for MCM-22.

Table 4. Deconvolution Data of ^{27}Al NMR Peaks for MCM-22 in Figure 1

ppm	angle	population
52.4	159.2	7
56.1	151.8	1
58.1	147.8	1
61.6	140.8	5

showing the number of Si atoms in different crystallographic T-sites), given in Table 6, were calculated (data for MCM-22-70 are presented), demonstrating a good agreement with experimental data.[46] However, other samples, not related to MCM-22, did not provide good spectral resolution, presumably because of amorphous structure.

In ^{29}Si CP/MAS spectra of MCM-22 a relative increase of the intensity in the region between −100 ppm and −110 ppm, was accompanied by the decrease in the intensity in the range of −111 and −120 ppm in the course of chemical modification. Also signals at −90 ppm became visible. An analogous picture was observed for MCM-48 catalysts, for example, increase of intensity between −100 ppm and −92 ppm, as well as intensity decrease for the shift at −108 ppm. The CP/MAS technique strongly and selectively enhances the peaks from hydroxylated sites and other silicons in their proximity: it additionally confirmed Q3 assignments for silanol groups.

Introduction of Pt in MCM-48 did not influence significantly on ^{29}Si spectra, although changes in intensities were observed. On the other hand changes in ^{27}Al spectra were noticeable, for example, decline in the absolute Al content (evidenced by signal-to-noise, S/N, ratio decrease), changes in the ratio between Al (IV) and Al (VI), as illustrated in the Table 7. The S/N data is only shown for MCM-48-derived mesoporous material.

3.2. Pulp Characterization Results. The degree of polymerization was determined to be equal to 1900. No products were detected in the water phase from the pulp-water suspension, indicating that no free monosaccharides were present in the raw material. The main monosaccharide detected from the acid methanolysis of the hemicelluloses was xylose, originating from xylans present in the pulp. The XRD from the fresh and used kraft pulp as well as pure cellulose are shown in Supporting Information, Figure S1.

dx.doi.org/10.1021/cs2006839 | ACS Catal. 2012, 2, 1381−1393

Table 5. ^{27}Al NMR Chemical Shift and Coordination Assignments for MCM-22-Based Zeolites

	chem. shift, ppm					
	−99.4	−105.5	−111	−114	−116	−120
coordination	Q3	Q4(4AI)	Q4(3AI)	Q4(2AI)	Q4(1AI)	Q4(OAI)
MCM-22-30	8.7	18.7	40.7	4.7	16.6	10.5
MCM-22-50	7.8	18.9	36.6	8.9	16.2	11.7
MCM-22-70	7.1	17.6	40.0	9.7	13.6	12.0

Table 6. Assignments of ^{29}Si Chemical Shifts for MCM-22-70 Zeolite

δ, ppm	T sites	population
−120.2	T1, T4, T5	1
−115.6	T6	1
−114.6	T3	1
−111.2	T7, T8	2
−106.3	T2	1

Table 7. Specification of Al in Pt/MCM-48 by ^{27}Al NMR

	Al(IV)/Al(VI)	Al(IV)	Al(VI)	S/N
MCM-48	7.4	88.0	12.0	40
Pt-MCM-48-IS	12.1	92.4	7.6	13
Pt-MCM-48-IE	3.1	75.5	24.5	27

Among the three samples, the pure Aldrich cellulose exhibited the highest crystallinity, while the kraft pulp showed the least crystallinity because of the presence of the less crystalline hemicelluloses. Noncatalytic experiments resulted in a crystallinity increase, because of the partial hydrolysis of hemicelluloses, which was observed with HPLC as formation of xylose and glucose. Being analyzed by TGA, the pure cellulose was the most stable, while the thermal stability increased for the kraft pulp after use in the noncatalytic experiments, because of the partial removing of the hemicelluloses (Supporting Information, Figure S2).

3.3. Product Characterization Results. *3.3.1. Determination of Unreacted Substrate.* The amount of unreacted substrate was determined by filtration of the unmodified cellulose/pulp, followed by drying and weighing. The quantity of dry unreacted cellulose compared to the amount of input material is reported in Table 8.

3.3.2. Total Organic Carbon (TOC) and pH. The total amount of carbon was measured in the liquid phase after the reaction time of 24 h, and the results are shown in Table 8. The results are displayed as percent of carbon dissolved in the liquid after 24 h in proportion to the total amount of carbon of the cellulose input, converted into glucose. High values were obtained with the two most acidic H-MCM-22 catalysts indicating that these materials were efficient in converting the nonsoluble cellulose into water-soluble products. The low value for the noncatalytic experiments indicates that a temperature of 458 K was inefficient for cellulose breakage. Luo et al have, however, reported that at temperatures above 478 K (H^+) ions are formed, capable of performing acid catalyzed hydrolysis of crystalline cellulose.[47] The acid formation is furthermore reversible, since the protons disappear automatically at ambient temperatures. Deguchi et al. reported that high temperature water solution above 673 K, at a pressure of 25 bar, is needed before the crystalline cellulose becomes amorphous and undergoes dissolution.[48] The highest TOC-value was obtained in the case of Pt-MCM-41 mesoporous material, evidencing its

Table 8. TOC and pH Measured for the Liquid at the End of the Experiment, along with Unreacted Cellulose and Calculated Mass Balance

catalyst	TOC, (%)	unreacted solid, (%)	carbon balance, (%)	pH, solution
		Aldrich Cellulose		
noncatalytic	26	69	95	3.80
H-MCM-22-30	39	34	73	3.26
		Birch Pulp		
noncatalytic	43	56	99	3.31
H-MCM-22-30	56	16	72	3.10
H-MCM-22-50	57	16	73	3.12
H-MCM-22-70	51	18	69	3.21
H-MCM-48	50	18	68	3.36
Pt-MCM-48-IE	55	16	71	3.55
Pt-MCM-48-IS	47	27	74	3.82
Pt-Al_2O_3	35	63	98	5.08
H-MCM-41	51	16	67	3.30
Pt-MCM-41	60	25	85	4.37
Al-SBA-15	52	21	73	3.34

excellent catalytic efficiency in converting the pulp into products stable in water. The noncatalytic experiments with pure cellulose gave lower values of dissolved carbon than the corresponding experiments with the kraft pulp. This can be explained by the fact that hemicelluloses in the kraft pulp are much more sensitive to thermo-mechanical treatment than pure cellulose with high crystallinity.[49] At the same time, Pt on Al_2O_3 exhibited an even lower value of dissolved carbon than the one in the noncatalytic experiment. This is most probably due to the monosaccharides which, although being found in minor amounts in the noncatalytic experiments, are further transformed into acids. This feature turns the system into a combination of homogeneous and heterogeneous catalysis and thus, enables a more efficient hydrolysis process.[49,50] The monosaccharides formed in the presence of Pt are, however, hydrogenated into sugar alcohols and have no additional effect on the hydrolysis. This sequence of reactions is in line with measured pH values of the solution at the end of the experiments (Table 8): the higher the Pt loading, the higher was the pH observed. The pH furthermore decreased in the following order: Pt-MCM-48-IS > Pt-MCM-48-IE > H-MCM-48, showing that the pH decreases linearly with decreasing platinum loading. The lowest pH was achieved with different microporous MCM-22 zeolites. The organic compounds that were not detectable with TOC refer not only to the unreacted cellulose but also to the tars which were formed on the reactor wall. Noteworthy, throughout the experiments there was some tar formation on the reactor walls which increased with reaction time.

3.3.3. Yield and Selectivity. Yield and selectivity of the most commonly formed products during hydrolysis and hydrolytic hydrogenation over the proton form and Pt modified catalysts

dx.doi.org/10.1021/cs2006839 | ACS Catal. 2012, 2, 1381−1393

Table 9. Yield (Y) and Selectivity (S) of formed Monosaccharides, Sugar Alcohols and Dehydration Products from Catalytic Transformation of Birch Kraft Pulp over Acid Zeolites, Proton and Pt-Modified Mesoporous Materials and Pt-Al_2O_3 at the End of the Experiments (reaction time 24 h)

	glucose		fructose		sorbitol		xylose		xylitol		5HMF		furfural		furfuryl alcohol	
catalyst	Y [%]	S [%]	Y [%]	S [%]	Y [%]	S [%]	Y [%]	S [%]	Y [%]	S [%]	Y [%]	S [%]	Y [%]	S [%]	Y [%]	S [%]
H-MCM-22-30[a]	6	14	2	4							3	8	1	2		
H-MCM-22-30	8	14	2	4			5	9			4	9	5	14		
H-MCM-22-50	8	14	2	3			5	9			4	10	5	15		
H-MCM-22-70	8	16	2	3			4	8			4	11	5	15		
H-MCM-48	14	28	2	4			4	7			8	21	9	27		
Pt-MCM-48-IE	5	8	2	3			3	3	1	2	5	13	3	8	1	3
Pt-MCM-48-IS	5	10	2	4	2	5	1	2	2	5	5	14	2	5	2	6
H-MCM-41	7	14	2	4			2	4			5	14	5	17		
Pt-MCM-41	1	1	1	1	10	12			4	5	1	2			1	2
Al-SBA-15	8	15	4	8			3	6			5	15	6	18		
Pt-Al_2O_3							1	4	7	18						

[a]Catalytic transformation of pure cellulose (Aldrich).

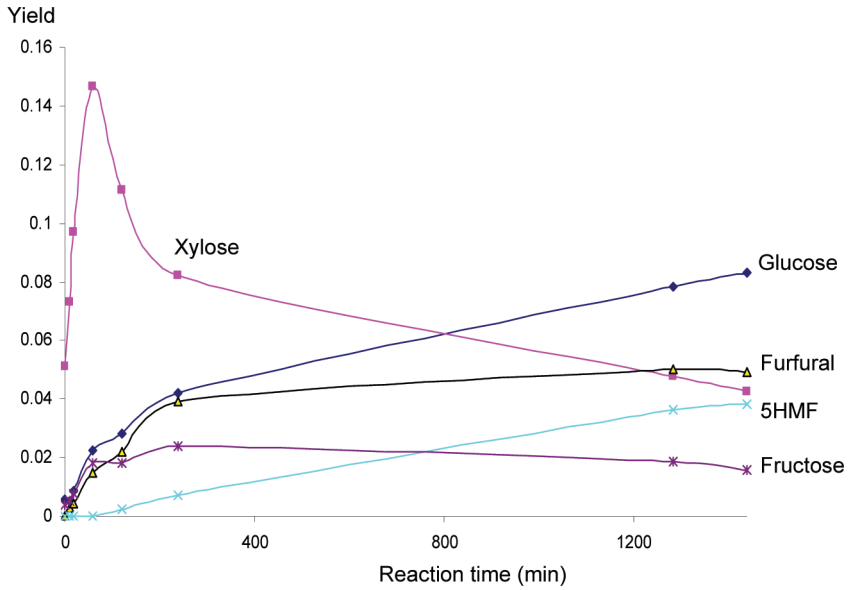

Figure 2. Formation of products from catalytic transformation of birch kraft pulp over H-MCM-22-70 microporous material.

were calculated based on the analysis results after a reaction time of 24 h (Table 9). The yields of the formed products were calculated as weight percent compared to the total amount of input substrate. The shown values for selectivity are reported as carbon selectivity in percent for each compound in relation to the total organic carbon measured in the liquid phase (Table 8). This means that the selectivity values indicate the carbon yield of the dissolved carbon.

The main products in transformations of kraft pulp over the microporous MCM-22 zeolite were xylose, glucose, furfural, 5HMF, and fructose (Table 9). There was no significant difference between the three MCM-22 zeolites with different acidities in terms of activity, as measured by conversion and selectivity even though there was a substantially difference in the acidity between the most acidic (MCM-22-30) and the least acidic (MCM-22-70) catalysts (Table 1). Xylose was the main product in the beginning of the experiments with a maximum yield detected after 60 min, followed by consecutive reactions (Figure 2). The sugar was formed at the initial stage of the experiment since the hemicelluloses in the birch kraft pulp, the xylans, are more easily hydrolyzed than the crystalline cellulose. At the end of the experiments glucose was the main product since the total amount of xylose present in the pulp had been dissolved and reacted further through consecutive reactions.

The detected products over the proton forms of the mesoporous material were xylose, glucose, fructose, 5HMF, and furfural (Table 9). In addition to the products detected over the proton form of MCM-48, sugar alcohols like xylitol and sorbitol as well as furfuryl alcohol were detected over the Pt modified mesoporous material (Figure 3). Higher amounts of sugar alcohols were seen over Pt-MCM-48-IS than over Pt-MCM-48-IE mesoporous catalyst in line with higher metal loading.

The products formed over the proton form of MCM-41 mesoporous materials were similar to those formed over the MCM-22 zeolites and the proton form of MCM-48 (Figure 4A). The selectivity as a function of conversion from catalytic transformations over H-MCM-41 mesoporous material is demonstrated in Figure 4B. The figure clearly indicates that xylose undergoes consecutive reactions. The molar yield of formed furfural as a function of the molar yield of the produced 5HMF in the catalytic transformations over microporous H-

dx.doi.org/10.1021/cs2006839 | ACS Catal. 2012, 2, 1381−1393

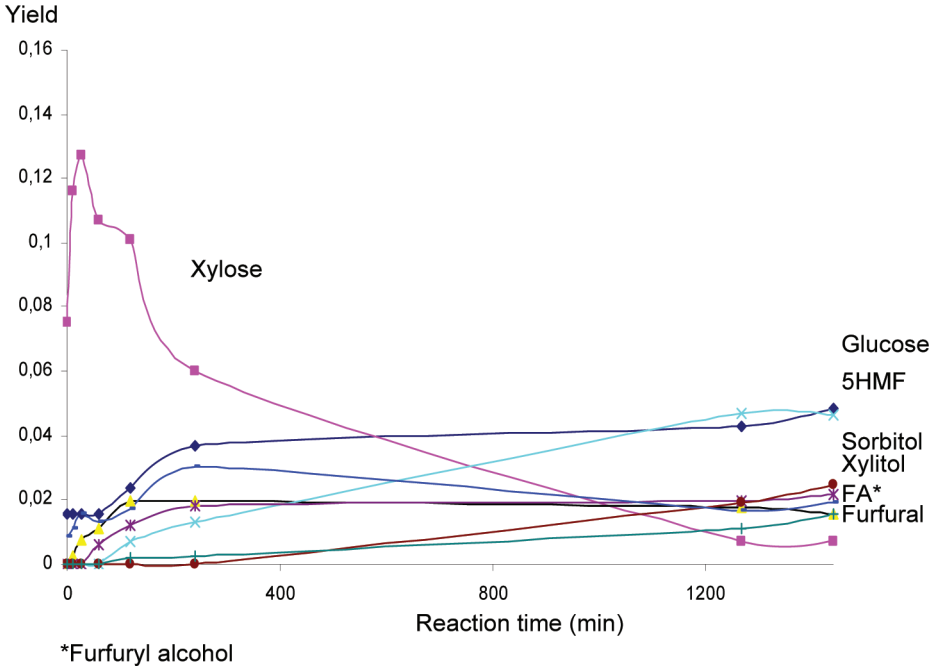

Figure 3. Formation of products from catalytic transformation of birch kraft pulp over Pt-MCM-48-IS mesoporous material.

MCM-22-50 as well as mesoporous H-MCM-41 and Pt-MCM-48-IS is presented in Figure 4C. Being more acidic than MCM-41, the microporous MCM-22 zeolite is more efficient in breaking down the crystalline cellulose which can be seen in the formation of 5HMF at an initial stage of the experiment over the MCM-22 microporous material. The formation of furfural from xylose is furthermore significantly lower over Pt modified MCM-48 compared to the proton form catalysts, because of the competing transformation of the pentose into xylitol.

The main product formed over Pt-Al_2O_3 was xylitol, indicating that all xylose formed was rapidly hydrogenated into the corresponding sugar (Table 9). Only traces of sorbitol were observed indicating that the catalyst was not able to hydrolyze cellulose, which can easily be understood since this catalyst lacks Brønsted acidity.[51] In addition small amounts of the sugars, mannose, sorbose, and galactose as well as the sugar alcohols such as mannitol and erythritol were detected. Similar results with low yields of glucose and sorbitol formed from catalytic transformations of birch kraft pulp over Ru on a nonacidic support (Ru/C) have recently been published.[52]

The highest amount of the sugar alcohols was detected over Pt-MCM-41 catalyst with the maximum yield of xylitol reaching 15 wt % of the original dry input pulp while the equivalent value of sorbitol was 11 wt % (Figure 5). The high value of xylitol indicates that all the formed xylose which could be traced to the xylans in the pulp, was hydrogenated into the corresponding sugar alcohol. Sundberg et al investigated the amount of monosaccharides originating from hemicelluloses in four different bleached birch pulps, identical to the substrate used in this work, from Finnish paper mills and found that the average amount of xylose in the pulps was 14.3 wt % (13.6–15.3%).[53]

Using the crystalline cellulose as feedstock, the main product formed was glucose with a maximum yield reaching 6 wt %. Other products detected where fructose originating from glucose isomerization, and dehydration products such as 5HMF, furfural, levulinic, and formic acid.

The overall yields of the formed products originating from the pulp and the crystalline cellulose are somewhat low under the investigated conditions, but they correspond well with the values reported by other groups.[10,54] Recent work has shown that cellulose pretreatment by ball milling makes it possible to reduce the crystallinity of the polymer and achieve higher yields of glucose and sorbitol.[55]

3.3.3.1. Volatile Compounds. The main volatile compound extracted with the CAR/PDMS fiber and detected with GC-MS was furfural (Supporting Information, Figure S3). The highest amount of this compound, according to the peak areas, was formed in the experiments with birch kraft pulp over H-MCM-22-30 microporous material and the proton form of MCM-48 mesoporous material. Among different MCM-48 catalysts the amount of detected furfural decreased in the following order: H-MCM-48 > Pt-MCM-48-IE > Pt-MCM-48-IS, indicating that the proton form dehydrated the sugars more efficiently than Pt containing materials. This can be accounted by the fact that xylose formed in the presence of Pt was partly hydrogenated into xylitol instead of being hydrolyzed into furfural.

Furfural was also observed in noncatalytic and catalytic transformations of pure cellulose, fructose, and glucose: even though the amounts were considerably lower than in experiments with the kraft pulp containing xylans. Furfural formed in experiments with pure cellulose and glucose originated most probably from decarbonylation of 5HMF.[56,57] The only catalyst over which furfural was not detected was Pt-Al_2O_3, since all xylose formed was hydrogenated into xylitol.

The main difference when comparing catalytic transformations of pure cellulose with birch kraft pulp over H-MCM-22-30 zeolite catalyst is the absence of xylose and consequently lower formation of furfural for the former substrate. Glucose was thereby the main product formed with the pure crystalline cellulose along with 5HMF and fructose.

3.3.4. Oligosaccharides. The retention times of the standard solution of acetylated α-D-glucose-pentaacetate (monosacchar-

dx.doi.org/10.1021/cs2006839 | ACS Catal. 2012, 2, 1381–1393

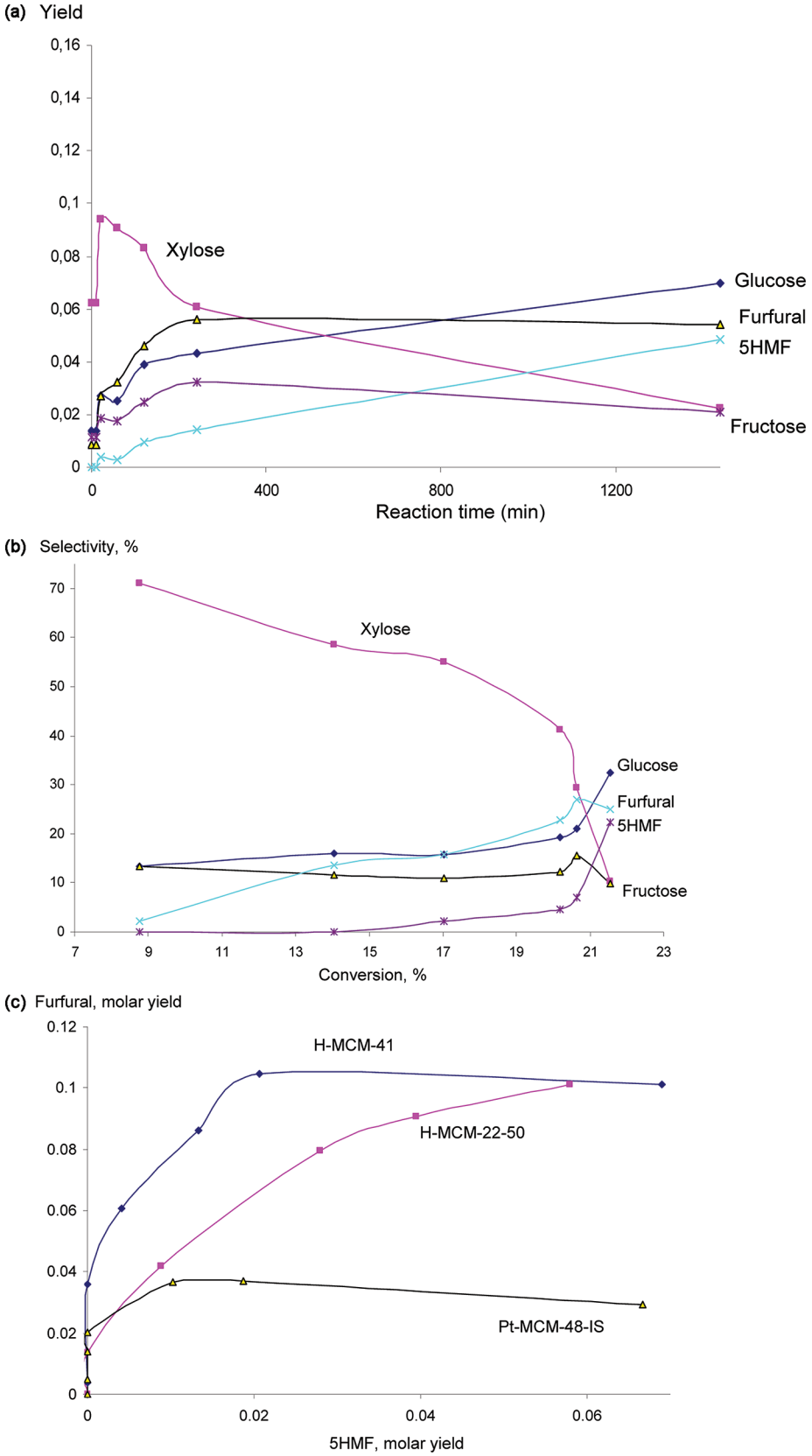

Figure 4. (a) Formation of liquid products from catalytic transformation of birch kraft pulp over H-MCM-41 mesoporous material. (b) Selectivity of liquid products from catalytic transformation of birch kraft pulp over H-MCM-41 mesoporous material. (c) The molar yield of furfural as a function of the molar yield of 5-HMF formed from catalytic transformation of birch kraft pulp over microporous H-MCM-22-50 and mesoporous H-MCM-41 and Pt-MCM-48.

dx.doi.org/10.1021/cs2006839 | *ACS Catal.* 2012, 2, 1381−1393

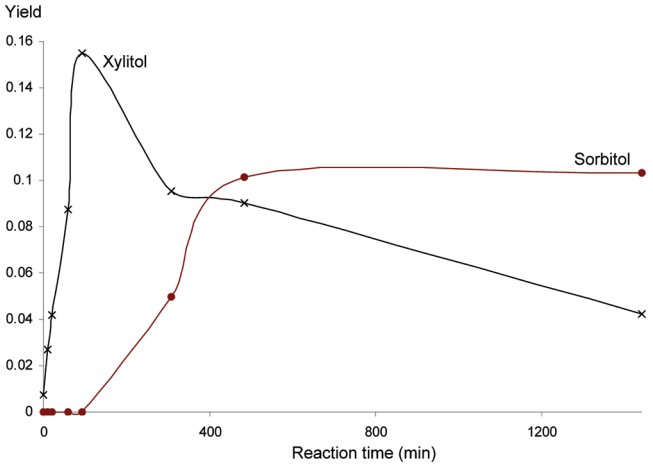

Figure 5. Formation of sugar alcohols from catalytic transformation of birch kraft pulp over Pt-MCM-41 mesoporous material.

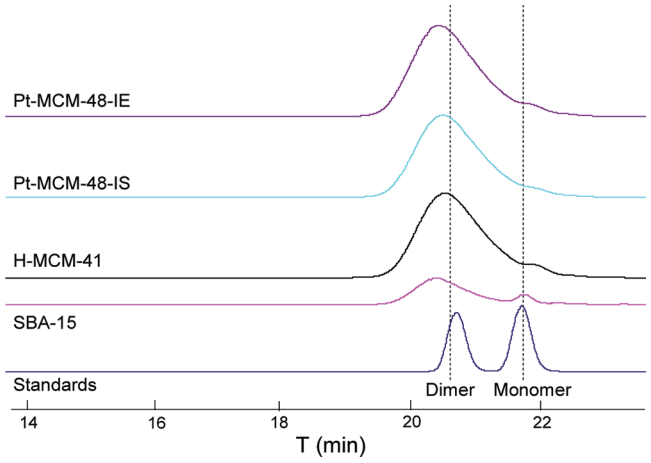

Figure 7. Formation of monomers and dimers in transformation of birch kraft pulp over different mesoporous materials.

ide) and D-cellubiose-octaacetate (disaccharide) were compared with that of the prepared samples. Samples from the catalytic transformation of both kraft pulp and pure cellulose were analyzed. Noncatalytic transformations as well as those over either microporous materials or Pt-Al_2O_3 catalyst yielded mainly products with retention times similar to the monomer standard (Figure 6). The signals were larger when catalysts were present for both kraft pulp and pure cellulose as reagents. This is natural since the catalysts are able to partly hydrolyze the polymers in the substrates. The use of Pt-Al_2O_3 catalyst resulted in the largest signal since the sugars formed were efficiently transformed into corresponding sugar alcohols, which were detectable by HPLC. The hydration of the sugars formed from transformation over the proton forms of microporous materials gave furfurals, which were vaporized during the sample preparation and not detectable with the ELS detector. Therefore the signal from transformation over Pt-Al_2O_3 catalyst was larger than the signals from the transformations over the microporous materials, even if the amount of total organic carbon in the solution was larger over the latter catalysts (Table 8).

The reaction over the mesoporous materials (MCM-48, MCM-41, SBA-15) resulted in larger amounts of disaccharides than monosaccharides (Figure 7). It seems that the mesoporous materials with their large pores enabled formation of larger molecules from the polymeric chains. Most probably very large cellulose molecules cannot enter the pores of the porous materials and interact with the acid sites. The acid sites in the pores may, however, contribute to the sequential reactions of hydrolyzed smaller molecules.

3.3.5. Carbon Balance. A carbon balance was calculated based on the values obtained from the total organic carbon analysis and the amount of unreacted solid cellulose/pulp (Table 8). The losses in the carbon balance are contributed to tars/humins attached to the reactor walls as well as to the formation of gaseous products. Comparing the values, the balance is most complete with the noncatalytic experiment as well as with the experiments using the two catalysts with the highest amounts of platinum (Pt-Al_2O_3 and Pt-MCM-41). This indicates that without a catalyst or when using a catalyst with high amount of Pt, low amounts of tars/humins and gaseous products are formed. This is understandable taking into consideration that the tars/humins are formed mainly from furan derivatives[58,59] and that the formation of furans and gaseous products from sugars both are promoted by presence of acidity but suppressed if hydrogenation is prominent.

3.4. Reaction Network. The reaction pathways based on the mechanistic understanding of hydrolytic hydrogenation

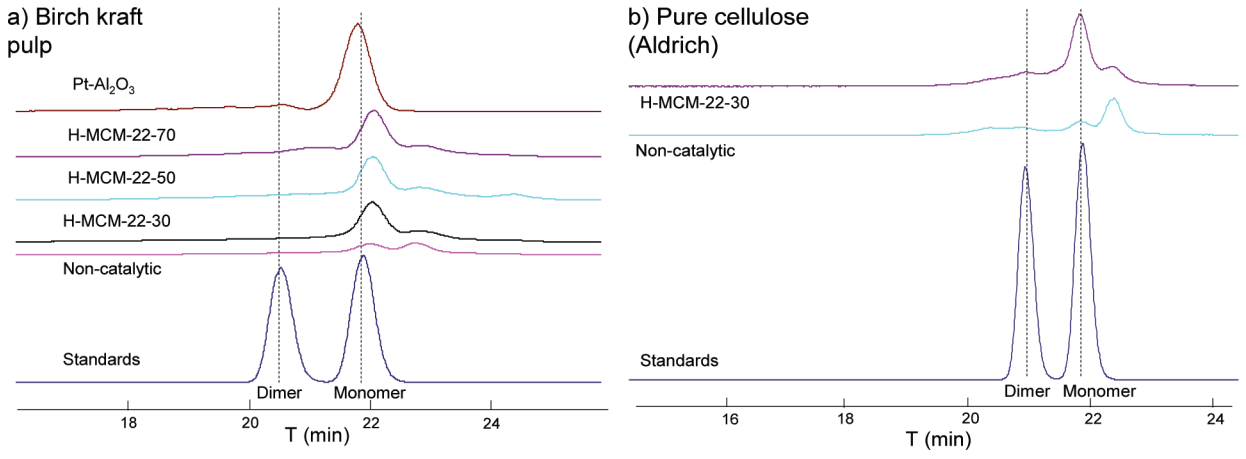

Figure 6. Formation of monomers and dimers in noncatalytic experiments, over microporous materials and Pt-Al_2O_3 in hydrolytic hydrogenation of (a) birch kraft pulp and (b) pure cellulose.

dx.doi.org/10.1021/cs2006839 | *ACS Catal.* 2012, 2, 1381−1393

Scheme 1. Reaction Network in Hydrolytic Hydrogenation of Bleached Birch Kraft Pulp

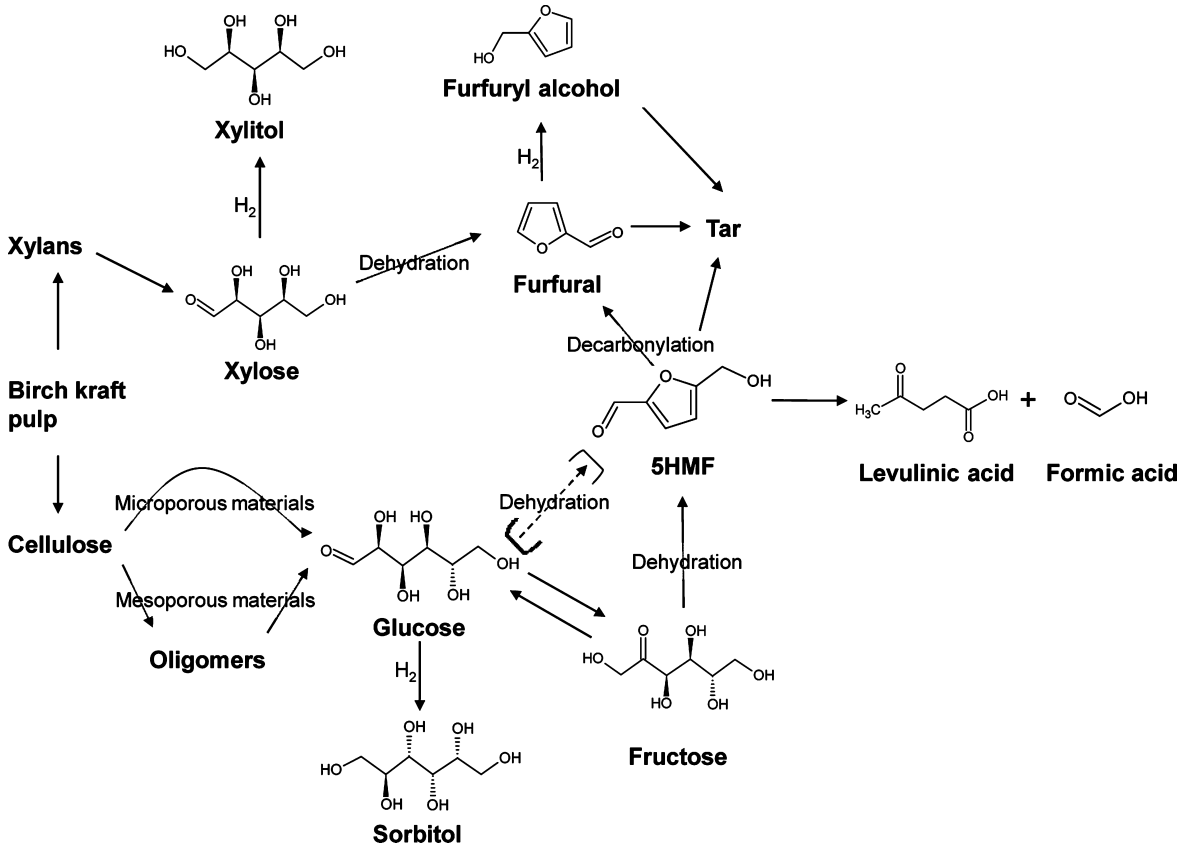

described in the literature and the current experimental data with the real birch pulp feedstock are shown in Scheme 1. The hydrolytic degradation of the bleached kraft pulp proceeds through two parallel reaction pathways, cellulose and the hemicellulose, xylan, as starting materials. Oligomers were detected in the catalytic transformations over mesoporous materials, and monosaccharides were consequently suggested to be formed through these intermediates. Since no oligomers were detected in the transformations over the microporous materials, the monosaccharides were suggested, in this case, to be formed from cellulose and hemicelluloses without intermediate release of oligomers into the reaction milleau. The breaking down of xylans leads to the formation of xylose, while the breaking down of cellulose gives glucose. The formation of xylose originates from the hemicelluloses in the pulp, since native birch wood (betula pendula) has been reported to contain 23% of xylose, bound in the form of the hemicellulose xylan.[60]

In the presence of Pt, the formed monosaccharides are hydrogenated into xylitol and sorbitol. The amount of Pt on the support is, however, crucial. If hydrolysis is the rate-limiting step in the reaction scheme, the formed sugars will be hydrogenated into sugar alcohols, whereas if hydrogenation is the rate-limiting step the sugars will be partly dehydrated into furfurals. The presence of furfural and 5HMF indicates thereby which reaction step is rate-limiting. 5HMF can furthermore be decarbonylated into furfural or broken down into levulinic and formic acid, and furfural, in turn, is hydrogenated into furfuryl alcohol. The scheme proposed shows that furfural can originate from both xylose and glucose. In addition formation of tar was also detected, a product most probably formed through the furan derivative intermediates.[58,59]

4. CONCLUSIONS

H-MCM-22 zeolite catalysts with varying acidities and H-MCM-41, H-MCM-48, and Al-SBA-15 mesoporous materials with different pore sizes and structures were synthesized and characterized. Pt was introduced in the MCM-48 mesoporous material using different methods, resulting in varying physicochemical and catalytic properties in the transformation of birch kraft pulp.

Assessment of catalytic properties was done in hydrolytic hydrogenation of bleached birch kraft pulp from a Finnish pulp mill and pure crystalline cellulose over synthesized materials as well over Pt on Al_2O_3 at 458 K and 20 bar of hydrogen. We show that the hemicellulose fraction in the pulp is much more easily hydrolyzed compared to the more crystalline cellulose, although the cellulose has lost some of its crystallinity because of the removal of lignin from the matrix. Xylose and glucose were the main monosaccharides formed with some sugar alcohols produced through hydrogenation of the corresponding sugars along with different furfural derivatives. We also show that although utilizing rather moderate temperatures some decarbonylation/decarboxylation of 5HMF into furfural is visible.

In contrast to experiments performed with microporous materials, formation of carbohydrate dimers over the mesoporous materials was observed and a reaction network was advanced. H-MCM-48 mesoporous material showed superior performance in yields of formed sugars and dehydration products compared to the other proton form

dx.doi.org/10.1021/cs2006839 | ACS Catal. 2012, 2, 1381−1393

catalysts. The carbon balance was the closest to being complete over the catalyst with high amount of platinum loading, as the metal loading was reduced or when utilizing the proton form catalysts, the formation of humins (tars) hampers the closure of a mass balance based on water-soluble products. We also point out the connection between pH and product distribution; a low pH of the water solution is an indication of formation of sugar dehydration products, whereas formation of sugar alcohols does not give a severe drop in pH. The pH was furthermore shown to decrease linearly with decreasing Pt loading on MCM-48. The presence of easily hydrolyzed xylans that goes through further dehydration gives also lower pH compared to experiments utilizing pure cellulose. The novelty of the work lies in the synthesis of Pt modified MCM-48 mesoporous material using different methods and its evaluation in the upgrading of real feedstock (birch kraft pulp) obtained from a pulp mill containing both cellulose and hemicelluloses. Furthermore the large combination of analytical techniques utilized for determining the different products was much more extensive than previously reported in the literature, enabling the formulation of the advanced reaction network.

■ ASSOCIATED CONTENT

Supporting Information

Further details are provided in Figures S1−S3. This material is available free of charge via the Internet at http://pubs.acs.org.

■ AUTHOR INFORMATION

Corresponding Author

*E-mail: dmurzin@abo.fi.

Funding

This work is part of the activities at the Åbo Akademi Process Chemistry Centre within the Finnish Centre of Excellence Programme (2000−2011) by the Academy of Finland.

Notes

The authors declare no competing financial interest.

■ ACKNOWLEDGMENTS

L. Österholm and S. Lindholm are acknowledged for the TOC and ICP-OES analysis, respectively.

■ REFERENCES

(1) Rinaldi, R.; Schüth, F. *Energy Environ. Sci.* **2009**, *2*, 610−626.
(2) Mohan, D.; Pittman, C. U.; Steele, P. H. *Energy Fuels* **2006**, *20*, 848−889.
(3) Gallezot, P. In *Catalysis for Renewables: From Feedstock to Energy Production*; Centi, G., van Santen, R. A., Eds.; Wiley-VCH Verlag GmbH & Co. KGaA: Weinheim, Germany, 2007; pp 53−73.
(4) Rinaldi, R.; Schüth, F. *ChemSusChem* **2009**, *2*, 1096−1107.
(5) Faith, W. L. *Ind. Eng. Chem* **1945**, *37*, 9−11.
(6) Dhepe, P. L.; Fukuoka, A. *ChemSusChem* **2008**, *1*, 969−975.
(7) Ji, N.; Zhang, T.; Zheng, M.; Wang, A.; Wang, H.; Wang, X.; Chen, J. G. *Angew. Chem., Int. Ed.* **2008**, *47*, 8510−8513.
(8) Fukuoka, A.; Dhepe, P. L. *Chem. Rec.* **2009**, *9*, 224−235.
(9) Deng, W.; Tan, X.; Fang, W.; Zhang, Q.; Wang, Y. *Catal. Lett.* **2009**, *133*, 167−174.
(10) Fukuoka, A.; Dhepe, P. L. *Angew. Chem., Int. Ed.* **2006**, *45*, 5161−5163.
(11) Dhepe, P. L.; Fukuoka, A. *Catal. Surv. Asia* **2007**, *11*, 186−191.
(12) Palkovits, R.; Tajvidi, K.; Procelewska, J.; Rinaldi, R.; Ruppert, A. *Green Chem.* **2010**, *12*, 972−978.
(13) Guha, S. K.; Kobayashi, H.; Hara, K.; Kikuchi, H.; Aritsuka, T.; Fukuoka, A. *Catal. Commun.* **2011**, *12*, 980−983.
(14) Van de Vyer, S.; Geboers, J.; Jacobs, P. A.; Sels, B. F. *ChemCatChem* **2011**, *3*, 82−94.
(15) Carlson, T. R.; Vispute, T. P.; Huber, G. W. *ChemSusChem* **2008**, *1*, 397−400.
(16) Mäki-Arvela, P.; Holbom, B.; Salmi, T.; Murzin, D. Yu. *Catal. Rev.* **2007**, *49*, 197−340.
(17) Mäki-Arvela, P.; Salmi, T.; Holmbom, B.; Willför, S.; Murzin, D. Yu. *Chem. Rev.* **2011**, *111*, 5638−5666.
(18) Zhou, C.-H.; Xia, X.; Lin, C.-X.; Tong, D.-S.; Beltramin, J. *Chem. Soc. Rev.* **2011**, *40*, 5588−5617.
(19) Lawton, S. L.; Leowicz, M. E.; Partridge, R. D.; Chu, P.; Rubin, M. K. *Microporous Mesoporous Mater.* **1998**, *23*, 109−117.
(20) Kresge, C. T.; Leonowicz, M. E.; Roth, W. J.; Vartuli, J. C. U.S. Patent 5098684, 1992.
(21) Geboers, J. A.; Stijn, V. V.; Ooms, R.; Beeck, B. O.; Jacobs, P. A.; Sels, B. F.
(22) Asensi, M. A.; Corma, A.; Martínez, A. *J. Catal.* **1996**, *158*, 561−569.
(23) Taguchi, A.; Schüth, F. *Microporous Mesoporous Mater.* **2005**, *77*, 1−45.
(24) Martín-Aranda, R. M.; Čejka, J. *Top. Catal.* **2010**, *53*, 141−153.
(25) Corma, A.; Corell, C.; Perez Pariente, J. *Zeolites* **1995**, *15*, 2−8.
(26) Zhao, D.; Feng, J.; Huo, Q.; Melosh, N.; Fredrickson, G. H.; Chmelka, B. F.; Stucky, G. D. *Science* **1998**, *279*, 548−552.
(27) Kumaran, G. M.; Garg, S.; Soni, K.; Kumar, M.; Sharma, L. D.; Dhar, G. M.; Rao, K. S. R. *Appl. Catal. A: Gen.* **2006**, *305*, 123−129.
(28) Aguado, J.; Calleja, G.; Carrero, A.; Moreno, J. *Chem. Eng. J.* **2008**, *137*, 443−452.
(29) Kresge, C. T.; Leonowicz, M. E.; Roth, W. J.; Vartuli, J. C. U.S. Patent 5098 684, 1992.
(30) Bernas, A.; Laukanen, P.; Kumar, N.; Mäki-Arvela, P.; Laine, E.; Holmbom, B.; Salmi, T.; Murzin, D. Yu. *J. Catal.* **2002**, *210*, 354−366.
(31) Pu, S. B.; Kim, J. B.; Seno, M.; Inui, T. *Microporous Mater.* **1997**, *10*, 25−33.
(32) Emeis, C. A. *J. Catal.* **1993**, *143*, 347−354.
(33) Baertsch, C. D.; Schmidt, M. A.; Jensen, K. F. *Chem. Commun.* **2004**, 2610−2611.
(34) Contreras-Andrade, I.; Vázquez-Zavala, A.; Viveros, T. *Energy Fuels* **2009**, *23*, 3835−3841.
(35) Massiot, D.; Fayon, F.; Capron, M.; King, I.; Le Calvé, S.; Alonso, B.; Durand, J. O.; Bujoli, B.; Gan, Z.; Hoatson, G. *Magn. Reson. Chem.* **2002**, *40*, 70−76.
(36) Viscosity in cupriethylenediamine solution, SCAN-CM, 15:99, 1999.
(37) Evans, R.; Wallis, A. F. A. *J. Appl. Polym. Sci.* **1989**, *37*, 2331−2340.
(38) Sundberg, A.; Sundberg, K.; Lillandt, C.; Holmbom, B. *Nord. Pulp Pap. Res. J.* **1996**, *11*, 216−219.
(39) Käldström, M.; Kumar, N.; Heikkilä, T.; Tiitta, M.; Salmi, T.; Murzin, D. Yu. *ChemCatChem* **2010**, *2*, 539−546.
(40) Käldström, M.; Kumar, N.; Heikkilä, T.; Murzin, D. Yu. *Biomass Bioenergy* **2011**, *35*, 1967−1976.
(41) Käldström, M.; Kumar, N.; Heikkilä, T.; Murzin, D. Yu. *Appl. Catal., A* **2011**, *397*, 13−21.
(42) Kubička, D.; Kumar, N.; Venäläinen, T.; Karhu, H.; Kubičkova, I.; Österholm, H.; Murzin, D. Yu. *J. Phys. Chem. B* **2006**, *110*, 4937−4946.
(43) Villegas, J. I.; Kubička, D.; Karhu, H.; Österholm, H.; Kumar, N.; Salmi, T.; Murzin, D. Yu. *J. Mol. Catal. A* **2007**, *264*, 192−201.
(44) Maheshwari, S.; Jordan, E.; Kumar, S.; Bates, F. S.; Penn, R. L.; Shantz, D. F.; Tsapatsis, M. *J. Am. Chem. Soc.* **2008**, *130*, 1507−1516.
(45) Engelhardt, G.; Radeglia, R. *Chem. Phys. Lett.* **1984**, *108*, 271−274.
(46) Leonowicz, M. E.; Lawton, J. A.; Lawton, S. L.; Rubin, M. K. *Science* **1994**, *264*, 1910−1913.
(47) Luo, C.; Wang, S.; Liu, H. *Angew. Chem.* **2007**, *119*, 7780−7783.
(48) Deguchi, S.; Tsuji, K.; Horikoshi, K. *Chem. Commun.* **2006**, 3293−3295.

(49) Li, H.; Saeed, A.; Sarwar, M. S.; Ni, Y.; van Heiningen, A. *J. Wood Chem. Technol.* **2010**, *30*, 48−60.
(50) Chang, C.; Ma, X.; Cen, P. Chin. *J. Chem. Eng.* **2009**, *17*, 835−839.
(51) Arve, K.; Hernández Carucci, J. R.; Eränen, K.; Aho, A.; Murzin, D. Yu. *Appl. Catal., B* **2009**, *90*, 603−612.
(52) Käldström, M.; Kumar, N.; Murzin, D. Yu. *Catal. Today* **2011**, *167*, 91−95.
(53) Sundberg, A.; Emet, S.; Rehn, P.; Vähäsalo, L.; Holmbom, B. *Proceedings of the 13th International Symposium on Wood and Pulping Chemistry*, Appita Inc.: Auckland, New Zealand, 2005; pp 361−365.
(54) Dhepe, P. L.; Ohshi, M.; Inagaki, S.; Ichikawa, M.; Fukuoka, A. *Catal. Lett.* **2005**, *102*, 163−169.
(55) Kobayashi, H.; Ito, Y.; Komanoya, T.; Hosaka, Y.; Dhepe, P. L.; Kasai, K.; Hara, K.; Fukuoka, A. *Green Chem.* **2011**, *13*, 326−333.
(56) Kato, K. *Agr. Biol. Chem.* **1967**, *31*, 657−663.
(57) Chauntanapum, A.; Matsumura, Y. *Ind. Eng. Chem. Res.* **2009**, *48*, 9837−9846.
(58) Titirici, M. M.; Antonietti, M.; Baccile, N. *Green Chem.* **2008**, *10*, 1204−1212.
(59) Chuntanapum, A.; Matsumura, Y. *Ind. Eng. Chem. Res.* **2009**, *48*, 9837−9846.
(60) Willför, S.; Sundberg, A.; Pranovich, A.; Holmbom, B. *Wood Sci. Technol.* **2005**, *39*, 601−617.